

RESEARCH ARTICLE

View Article Online

View Journal | View Issue



Cite this: *Inorg. Chem. Front.*, 2023, **10**, 6329

Diaspore as an efficient halide-free catalyst for the conversion of CO₂ into cyclic carbonates†

Antarip Mitra,^a Khushboo S. Paliwal,^a Sourav Ghosh,^a Saikat Bag,^a Avishek Roy,^a Aditi Chandrasekar^{*b} and Venkataramanan Mahalingam ^{*a}

Efficient fixation of carbon dioxide (CO₂) into epoxides under atmospheric pressure generally necessitates the use of halide ion-containing co-catalysts. However, the use of halide ion-containing materials as catalysts is less encouraged, particularly from an industrial point of view. This demands the development of a suitable halide-free catalyst for the successful fixation of CO₂ into epoxides to prepare cyclic carbonates under atmospheric pressure. In this work, we report diaspore [α -AlO(OH)] as an efficient halide-free catalyst for CO₂ fixation. Diaspore in the presence of a small amount of dimethyl formamide is able to convert a range of epoxides into their corresponding cyclic carbonates. Hardly any loss in the catalytic activity or change in the functional/chemical characteristics of diaspore was observed after five cycles. DFT calculations reveal the spontaneity of the diaspore-catalyzed cycloaddition reaction compared to that of the diaspore-free reaction. The stabilization of the substrates and intermediates on diaspore resulted in an overall negative change in Gibb's free energy of the reaction.

Received 19th July 2023,
Accepted 25th August 2023

DOI: 10.1039/d3qi01386c

rsc.li/frontiers-inorganic

Introduction

Carbon dioxide (CO₂) is the major contributor to greenhouse gases. There has been a huge surge in the CO₂ concentration in the atmosphere post industrial revolution. This results in many adverse impacts which include global warming, climate change and more.¹ CO₂ capture and their subsequent utilization as C₁ feedstock for the synthesis of various value-added chemicals is one of the sustainable ways to mitigate these excess CO₂ related challenges.² Among various reactions involving CO₂, the reaction of epoxides with CO₂ to produce cyclic carbonates has gained much attention.³ This is mainly ascribed to the advantageous atom-economical and non-reductive features of the pathway.⁴ In addition, cyclic carbonates are commercially important as they find significant applications like as electrolytes in lithium-ion batteries, in the preparation of vicinal diols, as high-boiling polar aprotic solvents, and more.^{5–7} However, the high activation energy for the cycloaddition reaction of CO₂ and epoxides necessitates the use of efficient catalysts in addition to the requirement of high temperature and pressure.^{8–11}

The rate-determining step of the reaction of epoxides with CO₂ to produce cyclic carbonates involves a nucleophilic attack to open the epoxide ring.^{12,13} Primarily, halide ions such as chlorides, bromides, or iodides are used to facilitate this ring-opening step.^{14–16} Moreover, hydrogen bond donors (*e.g.*, OH, –NH, and –COOH) or Lewis acidic centers (*e.g.*, metal ions) can assist this ring opening by increasing the electrophilicity of the epoxides.^{17–23} However, the corrosive nature of the halide ions limits their scope, particularly for scaling up synthesis from an industrial point of view. In this regard, halide-free heterogeneous catalysts have gained attention in recent years for the synthesis of cyclic carbonates.^{24,25} For instance, North and co-workers used salophens as catalysts to prepare cyclic carbonates using CO₂ under 10 bar pressure at 120 °C.²⁶ Similarly, Zhang *et al.* developed a homogeneous halide-free organocatalyst which catalyzed the cycloaddition reaction under 2 MPa pressure and at 120 °C.¹⁹ Recently, Ma *et al.* developed a halogen-free solid solution of CeO₂–ZrO₂ and explored CO₂ fixation into epoxides. The catalysis was performed at 150 °C under a CO₂ pressure of 6 MPa.²⁷ In another recent report, Bragato *et al.* developed ionic liquids to prepare cyclic carbonates at 120 °C under 2 MPa pressure of CO₂.²⁸ The above-mentioned works reported the halide-free synthesis of cyclic carbonates under high pressure. Nevertheless, to our knowledge, there are relatively few reports on halide-free heterogeneous catalysts to produce cyclic carbonates with satisfactory yields under atmospheric pressure. For instance, pyridyl salicylimines, ionic porous polymers and zinc MOFs have been used as catalysts for CO₂ fixation.^{17,24,29} Our group has recently developed a pyridine dicarboxylic acid coordinated to alu-

^aDepartment of Chemical Sciences, Indian Institute of Science Education and Research Kolkata, Mohanpur, West Bengal 741246, India.

E-mail: mvenkataramanan@yahoo.com

^bSchool of Arts and Sciences, Azim Premji University, Bangalore 562125, India.

E-mail: aditi.chandrasekar@apu.edu.in

† Electronic supplementary information (ESI) available. See DOI: <https://doi.org/10.1039/d3qi01386c>

minium as a heterogeneous catalyst for CO₂ fixation under halide-free conditions.³⁰ However, the developed Al-based material was amorphous in nature. In this context, our idea is to use aluminium oxyhydroxide [AlO(OH)] as it is a stable material and can be easily prepared. In addition, AlO(OH) has been used in various applications like as sensors, adsorbents, batteries, in gas separation, *etc.*^{31–35} However, it is less explored as a catalyst, particularly for CO₂ fixation reactions.^{36,37}

This work reports the utilization of diaspore [α -AlO(OH)] as an efficient catalyst for the synthesis of cyclic carbonates from epoxides under ambient CO₂ pressure. Diaspore was prepared through a facile synthetic method, *i.e.*, by reacting Al(NO₃)₃·9H₂O and urea in water. The as-prepared diaspore in the presence of a small amount of DMF successfully converted different epoxides into their corresponding cyclic carbonates with high selectivity and quantitative yields. In addition, the material retained its activity for five cycles of catalysis. Theoretical calculations using DFT suggested the stabilization of intermediates by Al(III) ions resulting in the negative Gibb's free energy change of the reaction.

Experimental section

Synthesis of diaspore [α -AlO(OH)]

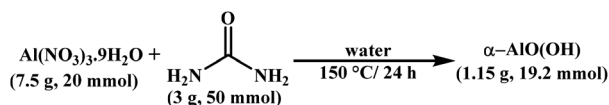
Diaspore was prepared using Al(NO₃)₃·9H₂O and urea in water (Scheme 1).³⁸ Briefly, Al(NO₃)₃·9H₂O (7.5 g, 20 mmol) and urea (3 g, 50 mmol) were dissolved in a round bottom flask containing 50 ml of water. The solution was heated at 150 °C for 24 hours. The solution was cooled, and the white precipitate was washed with water and acetone. The white precipitate was washed with water and acetone. The material was finally dried by overnight heating at 60 °C in a hot air oven followed by vacuum drying in a desiccator (1150 mg; yield 95.8%).

CO₂ cycloaddition

The reactions were performed in a 25 ml Schlenk round-bottom flask.¹⁴ Epichlorohydrin (12.75 mmol, 1.0 ml) or other epoxides were added along with diaspore (60 mg, 1 mmol). The setup was connected to a CO₂ balloon (99.5% pure) and heated at 100 °C for 24 hours. After the completion of the reaction, 20 μ l of the reaction mixture was dissolved in 600 μ l of CDCl₃ and the ¹H-NMR spectrum was recorded to calculate the conversion.

Hot filtration test

The hot filtration test for the catalysis was performed by removing the catalyst AlO(OH) through filtration after 6 h of reaction. Following the filtration, the filtrate was further



Scheme 1 Schematic protocol for the synthesis of diaspore [α -AlO(OH)] in aqueous medium.

allowed to react with CO₂ under optimized conditions for another 10 h in the absence of catalysts. The conversion of the final catalyst-free reaction mixture was compared with the conversion of the reaction mixture using AlO(OH) as a catalyst.

Computational strategy

Throughout the study, the ORCA 5.0.1 electronic structure program was used to optimize the geometries and compute the binding free energies.^{39,40} These calculations are extremely helpful and serve to provide valuable insights into the experiments carried out in this study. The geometries were optimized within the framework of DFT by employing the PBE functional in conjunction with the def2-TZVP basis set.^{41–44} For the calculations containing a diaspore sheet, a constrained optimisation has been employed, in order to maintain the planarity of the [0 4 0] catalytic surface. All the reactant and product geometries have been verified as minima by computing their harmonic vibration frequencies using the NUMFREQ module. Transition states have been optimized using the surface scans and transition state optimization protocols as implemented in ORCA. The transition state has been verified by computing the vibrational frequencies. The solvent effects were computed within the conductor-like polarizable continuum model (CPCM) using the default radii of all atoms. For these, a dielectric constant of 22.6 was used to mimic the reaction conditions. A similar protocol has been followed before and yielded computational results that matched well with the experiments.³⁸ Charges on the relevant atoms within the molecules before and after binding to alumina have been calculated using the Mulliken population analysis.

Results and discussion

Characterization

The PXRD pattern of the as-prepared diaspore matched well with the corresponding standard pattern (Fig. 1a, ICDD no. 00-001-1284). The diaspore is stable in polar and non-polar solvents such as ethanol, hexane, dimethyl sulfoxide (DMSO), DMF, and dichloromethane. This is supported by the PXRD patterns collected after the diaspore was stirred in the above-mentioned solvents for 12 h and subsequently dried (Fig. S1†). In addition, the prepared diaspore is stable in a wide pH range of 1 to 12 as confirmed by the PXRD results (Fig. S2†). The Brunauer–Emmett–Teller (BET) surface area of the prepared diaspore is found to be 75.9 m² g⁻¹. The results reveal the type-IV isotherm, confirming the mesoporous nature of the material. The observed type H1 hysteresis loop proves the presence of a narrow range of uniform mesopores with ink-bottle pore geometry (Fig. 1b).⁴⁵ The porosity was found to be 30.66%. The CO₂ adsorption of the as-prepared diaspore was found to be 5.38 cm³ g⁻¹, which confirms the moderate affinity of the material towards CO₂ (Fig. 1c). Although the CO₂ adsorption value is smaller compared to those of porous materials such as MOFs, porous polymers, *etc.*,^{23,46} the obtained value is better than those of nanoparticle catalysts

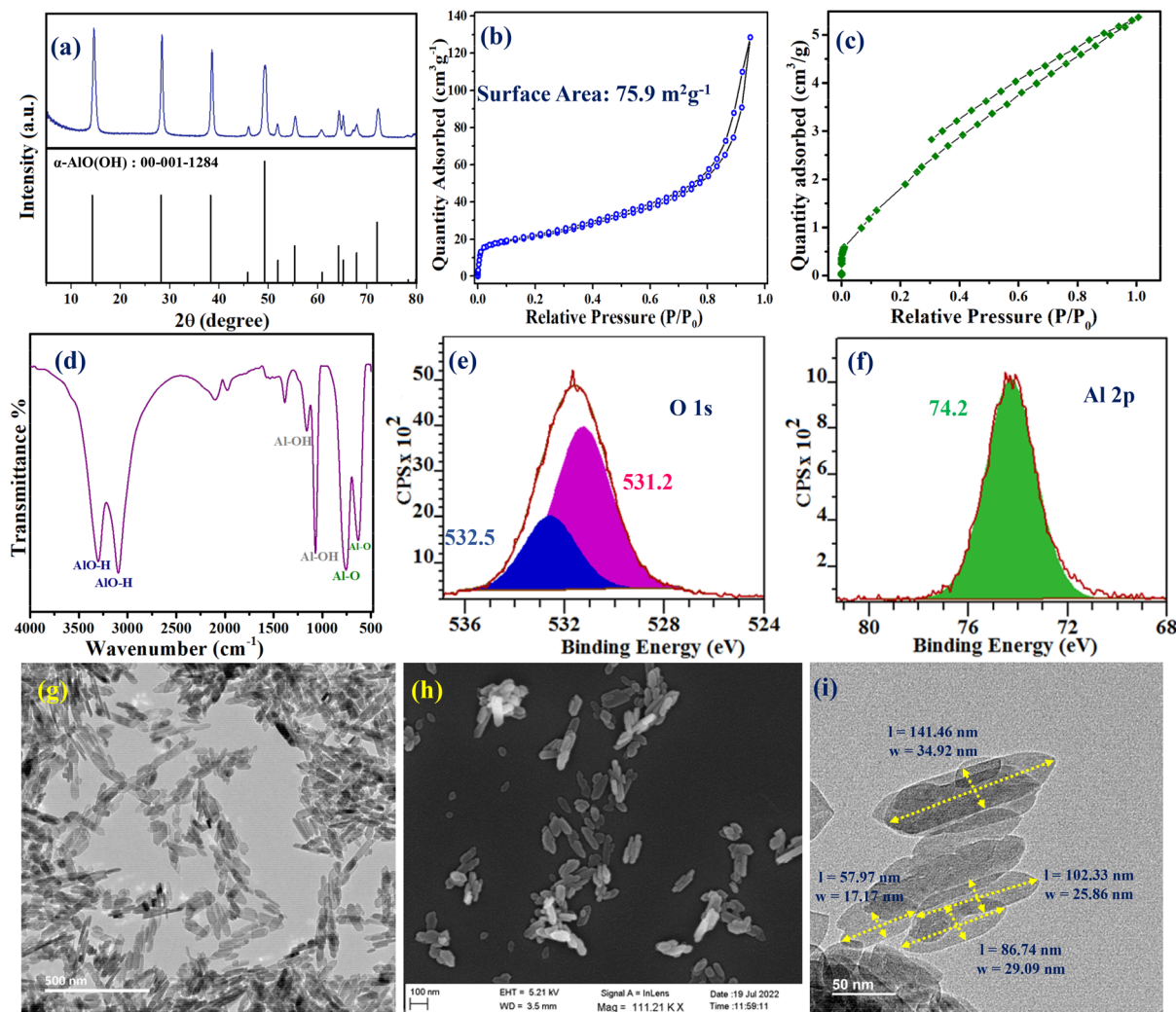


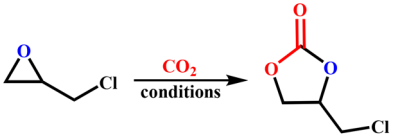
Fig. 1 Characterization of diaspore: (a) PXRD patterns; (b) N_2 gas adsorption–desorption isotherm; (c) CO_2 gas adsorption–desorption isotherm; (d) FT-IR spectrum; (e) O 1s XPS spectrum; (f) Al 2p XPS spectrum; and (g–i) FESEM and TEM images.

such as Fe_2O_3 , Al_2O_3 , and SiO_2 .^{38,47,48} The FT-IR spectrum of the sample showed two sharp bands at 3300 cm^{-1} and 3100 cm^{-1} . These two bands are assigned to the asymmetric and symmetric stretching of the O–H bonds of $AlO(OH)$, respectively (Fig. 1d). Another sharp band at 1070 cm^{-1} corresponding to the Al–OH bending vibrations is noted. The bands corresponding to the Al–O bonds are observed at 760 and 630 cm^{-1} .⁴⁹ X-Ray photoelectron spectroscopy (XPS) analysis was performed to understand the chemical states of the elements in $\alpha\text{-AlO(OH)}$. The O 1s spectrum was deconvoluted into two components with the binding energy maxima at 531.2 eV and 532.5 eV . The peak at 531.2 eV is the peak for the Al–O–Al units, while the peak at 532.5 eV corresponds to the Al–OH bonds (Fig. 1e). The Al 2p spectrum has a sharp peak at 74.2 eV which is a characteristic signal of $AlO(OH)$ compounds (Fig. 1f).⁵⁰ The morphology of the developed diaspore was studied using FESEM and TEM analyses. The FESEM images of the as-prepared material reveal the formation of grain like

morphology (Fig. 1g). This suggests that grains observed in SEM images consist of a large number of lamellae (Fig. 1h). The TEM images reveal the formation of a quasi-quadrangular prism shaped morphology. The lamellae possess lengths ranging from 58 nm to 140 nm and widths varying from 18 nm to 35 nm (Fig. 1i).⁵¹ The EDS and mapping analyses imply uniform Al and O distribution throughout the surface (Fig. S3†).

Optimization of the CO_2 fixation reaction

The catalytic efficiency of diaspore towards CO_2 fixation was evaluated using epichlorohydrin as the model substrate. First, a blank reaction was conducted in the absence of catalysts (only epoxide and CO_2) and hardly any conversion was noted (Table 1, entry 1). The reaction of epichlorohydrin (1.0 mL , 12.75 mmol) and diaspore (60 mg , 1 mmol) resulted in 58% conversion (entry 2, Fig. S4†). To increase the conversion, N,N' -dimethyl formamide (DMF) was used as it could assist the acti-

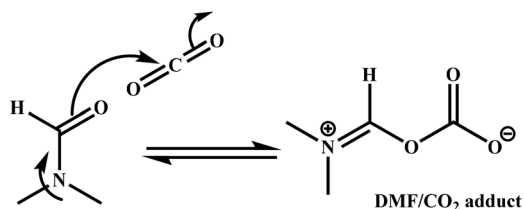
Table 1 Effect of reaction parameters on the coupling of CO₂ and epichlorohydrin


Entry	Catalyst used	Conversion
1	No catalyst	No reaction
2	α -AlO(OH)	58%
3	α -AlO(OH) + DMF ^a	>99%
4	α -AlO(OH) + DMF ^b	>99%
5	α -AlO(OH) + DEF ^b	>99%
6	α -AlO(OH) + DMAc ^b	92%
7	α -AlO(OH) + 3-methyl butanone ^b	58%
8	α -AlO(OH) + 2-methyl propanal ^b	58%
9	DMF ^a	Traces
10	DEF ^a	Traces
11	DMAc ^a	Traces
12	Al(NO ₃) ₃ ·9H ₂ O	<1%
13	Al(NO ₃) ₃ ·9H ₂ O + DMF ^a	12%

Conditions: 1 ml of epichlorohydrin (12.75 mmol), 60 mg of α -AlO(OH), 100 °C, 24 h, and 1 atm CO₂. ^a12.75 mmol of reagents. ^b0.25 mmol of reagents.

vation of CO₂ through the formation of a DMF/CO₂ adduct (Scheme 2).^{19,52} Addition of 12.75 mmol (~1 ml) of DMF resulted in almost complete conversion of equimolar epichlorohydrin (12.75 mmol, 1.0 ml) at 100 °C and 24 hours (entry 3, Fig. S5†). When the molar concentration of DMF was reduced to one-fifth (0.25 mmol) of the epoxide concentration, complete conversion was observed under similar conditions (entry 4). Furthermore, DMF also served as an internal standard to calculate the selectivity of the reaction from NMR analysis (Fig. S5†).

When other amides like *N,N'*-diethyl formamide (DEF, 0.25 mmol) and *N,N'*-dimethyl acetamide (DMAc, 0.25 mmol) are used instead of DMF for the CO₂ fixation reaction with diaspore, similar conversions are observed (entries 5 and 6, Fig. S6†). To understand the role of carbonyl groups, similar reactions were performed using 3-methylbutan-2-one (ketone, the carbon analogue of DMAc) and 2-methylpropanal (aldehyde, the carbon analogue of DMF). However, only 58% conversion was noted when the combination of diaspore and the above aldehyde/ketone was used (entries 7 and 8). This value is similar to that obtained for the reaction with only diaspore,

**Scheme 2** Reaction of DMF with CO₂ for the formation of the DMF/CO₂ adduct.

suggesting that the carbonyl functional groups of the aldehydes or ketones have hardly any role in the catalytic activity. These results clearly indicate that amides (*e.g.*, DMF or DMAc) play an important role in enhancing the catalytic activity of diaspore. However, individually DMF, DEF and DMAc are not capable of catalysing the reaction of epichlorohydrin and CO₂ (entries 9–11). In addition, the catalytic activity of the precursor of diaspore, *i.e.*, Al(NO₃)₃·9H₂O, is very low as the conversion is quite negligible (entry 12). The combination of DMF and Al(NO₃)₃·9H₂O was able to convert only 12% epichlorohydrin (entry 13).

The effect of temperature and time was also evaluated for the optimization of reaction conditions. Reactions were performed at different temperatures ranging from 70 to 115 °C and almost full conversion occurred at 100 °C (Fig. 2a). Similarly, the aliquot of the reaction mixture was collected at intervals of 8, 12, 16, 20, and 24 hours to check the corresponding conversions. The results confirmed the complete conversion of epichlorohydrin at 16 h (Fig. 2b). Based on the above observations, the reactions (substrate scope) were performed at 100 °C for 16 h using 1 ml of epichlorohydrin, 60 mg of diaspore, and 0.25 mmol of DMF. The turnover number (TON) for this reaction was found to be 12.75.

In addition to the above results, further optimization was performed using a halogen-free epoxide like styrene oxide. The results as tabulated in Table 2 show 64% conversion of 12.75 mmol of the epoxide using 60 mg of AlO(OH) at 100 °C and 24 hours (entry 2, Fig. S7†). For the complete conversion of styrene oxide, different concentrations of amides like DMF (12.75 mmol and 0.25 mmol) were used under similar conditions and complete conversion was observed (entries 3 and 4). To understand the effect of temperature, reactions were performed at lower temperatures of 70 and 85 °C, which resulted in 13% and 55% conversion, respectively (entries 5 and 6). Similarly, reactions were performed for a shorter duration of time at 100 °C in the presence of AlO(OH) and DMF. To optimize the reaction time, cycloaddition reactions were performed for different durations. After durations of 8 and 12 h, 44% and 60% styrene oxide were converted to styrene carbonate (entries 7 and 8). The complete conversion was noted when the reaction was performed at 100 °C for 16 h (entry 9, Fig. S8†). The above results indicate that the optimized con-

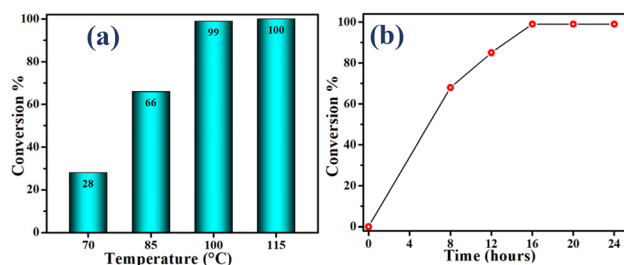
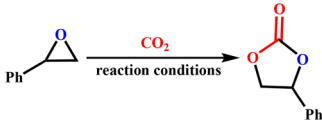
**Fig. 2** Reaction optimization: (a) bar diagram depicting the increase in the CO₂ conversion with an increase in the temperature of the reaction and (b) graph shows the effect of reaction duration on the conversion.

Table 2 Effect of reaction parameters on the coupling of CO₂ and styrene oxide


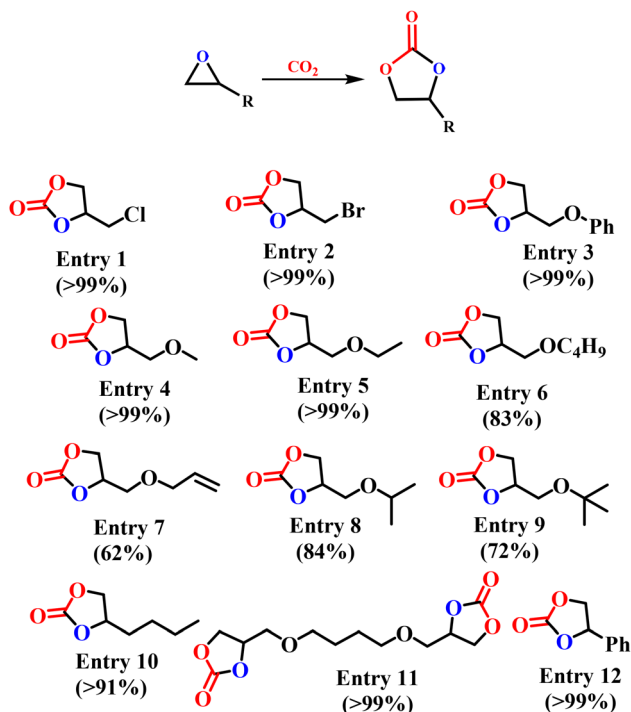
Entry	Catalyst used	Temperature, time	Conversion
1	No catalyst	100 °C, 24 h	No reaction
2	α-AlO(OH)	100 °C, 24 h	64%
3	α-AlO(OH) + DMF ^a	100 °C, 24 h	>99%
4	α-AlO(OH) + DMF ^b	100 °C, 24 h	>99%
5	α-AlO(OH) + DMF ^b	85 °C, 24 h	55%
6	α-AlO(OH) + DMF ^b	70 °C, 24 h	13%
7	α-AlO(OH) + DMF ^b	100 °C, 8 h	44%
8	α-AlO(OH) + DMF ^b	100 °C, 12 h	60%
9	α-AlO(OH) + DMF ^b	100 °C, 16 h	>99%

Conditions: 1.45 ml of styrene oxide (12.75 mmol), 60 mg of α-AlO(OH), and 1 atm CO₂. ^a 12.75 mmol of DMF. ^b 0.25 mmol of DMF.

ditions are similar for both the epoxides (epichlorohydrin and styrene oxide).

Substrate scope

The catalytic efficiency of diaspore was examined using different epoxides (Scheme 3). Epoxides having electronegative



Scheme 3 Diaspore catalyzed cycloaddition of CO₂ with epoxides. Reaction conditions: epoxides (12.75 mmol), CO₂ (1 atm), diaspore (1 mmol, 60 mg), DMF (0.25 mmol, 0.2 ml), 100 °C, 16 h. Conversions are calculated using ¹H-NMR spectroscopy.

heteroatoms such as epichlorohydrin and epibromohydrin showed almost complete conversion (entries 1 and 2). The observed higher conversion could be attributed to the presence of electronegative heteroatoms such as chlorine and bromine which could stabilize the electron-rich intermediate. Similarly, epoxides such as phenyl glycidyl ether, methyl glycidyl ether and ethyl glycidyl ether containing electronegative oxygen atoms displayed almost complete conversion (entries 3–5, Fig. S9†). Epoxides containing longer hydrocarbon chains such as glycidyl *n*-butyl ether and allyl glycidyl ether showed 83% and 62% conversion, respectively (entries 6 and 7, Fig. S10 and S11†). The catalyst was able to convert epoxides such as isopropyl glycidyl ether and *tert*-butyl glycidyl ether which contain bulky alkyl groups to the corresponding cyclic carbonates (entries 8 and 9, Fig. S12 and S13†). 1,2-Epoxy hexane was also converted at an efficiency of 91% (entry 10, Fig. S14†). Diepoxides such as 1,4-butanediol diglycidyl ether showed complete conversion under the optimized conditions (entry 11, Fig. S15†). Styrene carbonate is an industrially important compound which is used as an electrolyte for batteries, synthesis of aromatic carbamates, vicinal diols, *etc.*^{6,53} Nearly complete conversion is noted for the CO₂ fixation of styrene oxide using diaspore (entry 12). Additionally, to check the selectivity, the isolated yields of seven different cyclic carbonates were calculated, and they are found to be almost similar to the conversions calculated from ¹H-NMR spectroscopy (Table S1 and Fig. S16–S23 in the ESI†). The above observations indicate the high selectivity of the catalyst and the negligible possibility for the formation of other side products. Table S2 (ESI†) shows the comparison of the catalytic activity of the diaspore with other halide-free catalysts reported in the literature. Most of the heterogeneous catalysts reported the conversion of fewer epoxides under atmospheric pressure. Diaspore (this work) is able to convert twelve epoxides to their corresponding cyclic carbonates under atmospheric pressure with reasonable yields.

Recyclability study of the catalyst

After the completion of the reaction of diaspore with the above-mentioned epoxides, the diaspore was recovered from the reaction mixtures. To recover the catalyst, the reaction mixture was washed with ethyl acetate and the solid catalyst was separated by centrifugation (4000 rpm for 5 minutes). The separated diaspore was washed with acetone and dried in a hot air oven, followed by keeping it in a vacuum desiccator for 6 hours. The PXRD pattern of the recovered samples matched the standard pattern of diaspore, as shown in Fig. S24.† The above results confirmed the recovery of diaspore after one cycle of catalysis. To further study the reusability of diaspore for multiple cycles, the reaction between styrene oxide (1.45 ml, 12.75 mmol) and CO₂ was performed using the combination of diaspore (60 mg, 1 mmol) and DMF (0.25 mmol) under the above optimized conditions (Fig. 3a). After the completion of each catalytic cycle, the catalyst (diaspore) was recovered in the above-mentioned protocol and subsequently used for the next catalytic cycle. Hardly any change in the activity of

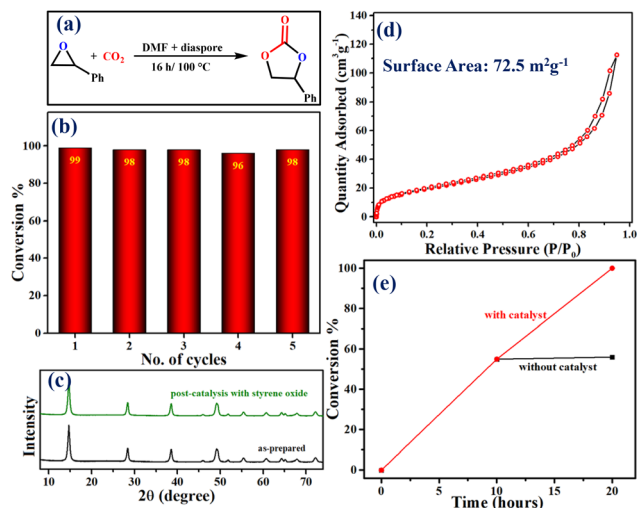


Fig. 3 Recyclability: (a) model reaction for recyclability studies; (b) bar diagram indicating the high recyclability of the catalyst; (c) PXRD comparison of the original sample and the post-catalytic material; (d) N_2 gas adsorption–desorption isotherms; and (e) hot-filtration test.

the catalytic combination is noted up to five cycles, suggesting that diaspore is highly recyclable for the cycloaddition reaction (Fig. 3b and Fig. S25[†]). The PXRD pattern of the recovered material after the fifth cycle matched well with the pattern of the as-prepared diaspore (Fig. 3c). The results further proved diaspore to be stable in different cyclic carbonates and can be reused for multiple cycles of catalysis. BET analysis indicates that the surface area ($72.5 \text{ m}^2 \text{ g}^{-1}$) of the recovered material is close to the corresponding value of the pre-catalyst ($75.9 \text{ m}^2 \text{ g}^{-1}$), suggesting the retention of mesoporosity of the catalytic network (Fig. 3d). This is further supported by the TEM images showing the retention of the grain-like morphology even after five cycles of catalysis (Fig. S26[†]). A hot-filtration test is another technique to check the heterogeneous behavior of the catalyst. The stability of diaspore was studied through a hot-filtration test (as explained in the Experimental section). The reaction of styrene oxide with CO_2 for 10 h using diaspore at 100°C resulted in 55% conversion. Following this, the catalyst was separated from the reaction mixture and the catalyst free reaction mixture was heated for another 10 hours at 100°C , and no further conversion was observed (Fig. 3e). The above results revealed the non-leaching of Al(III) ions from diaspore which further proved the robust nature of diaspore and the heterogeneous catalytic behavior. To check the leaching of aluminium ions into the reaction mixture, inductively coupled plasma atomic emission spectroscopy (ICP-AES) of the reaction mixture was performed. The aliquots from the reactions of epichlorohydrin with CO_2 (Scheme 3, entry 1) and styrene oxide (Scheme 3, entry 12) with CO_2 were collected for evaluation. As shown in Table S3 of the ESI,[†] there was an absence of Al(III) ions in the reaction mixture. The above observations proved the non-leaching of Al(III) ions into the reaction mixture during the course of the reaction.

Computational results

The experimental results show that the CO_2 insertion reaction does not occur in the presence of DMF alone. Nevertheless, in the presence of diaspore and DMF, the reaction takes place, and the cyclic carbonate is formed as the product. As the spontaneous occurrence or non-occurrence of a reaction is governed by the change in Gibb's free energy associated with the reaction, the computational studies focus on this aspect. The free energy change associated with the reaction mechanism, both in the presence and absence of diaspore, has been separately investigated in this light.

Diaspore free mechanism and energetics of CO_2 insertion

Fig. 4 shows the optimized geometries of the reactants and products at each stage of the reaction. Considering Str. I as zero energy, the free energy (kcal mol^{-1}) of each geometry (Str. II to IV) is indicated in the inset. The first step involves the addition of carbon dioxide to DMF, yielding structure II with the carbon dioxide forming an adduct with DMF. The next step is the addition of epoxy chloride. The epoxy ring opening and its addition to the DMF- CO_2 adduct do not yield a stable geometry. There is only a transition state geometry formed and this is hence indicated by the dashed line below structure III. The final step is ring closure yielding the cyclic carbonate with the elimination of DMF. The first two steps are endergonic and the last step is exergonic. The overall free energy change of the reaction is positive ($+19.5 \text{ kcal mol}^{-1}$), rendering the complete reaction non-spontaneous.

Energetics of CO_2 insertion in the presence of diaspore

Fig. 5 shows the geometry minima stabilized on the diaspore [0 4 0] surface. The interactions between the oxygen atoms of the substrates and diaspore (Al...O) are indicated. The corresponding interaction distances are included in the inset of Fig. 5. The lowest energy geometries have been considered

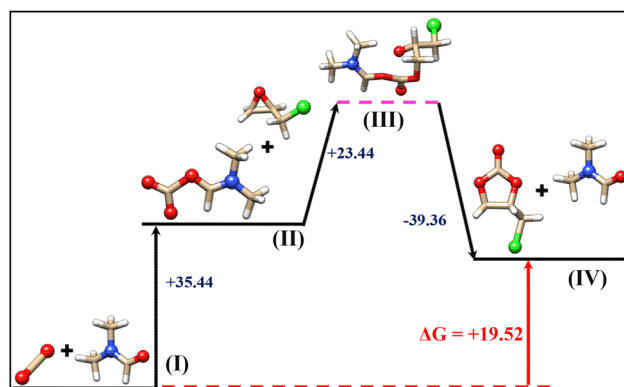


Fig. 4 Representation of the relative energies (kcal mol^{-1}) corresponding to those of (I) DMF and CO_2 , (II) their DMF + CO_2 adduct, (III) a transition state where the halo alkoxide binds the adduct, and (IV) cyclic carbonate product on the elimination of DMF. The transition state is indicated by a dotted line drawn below the structure. The net free energy change for the entire reaction is indicated.

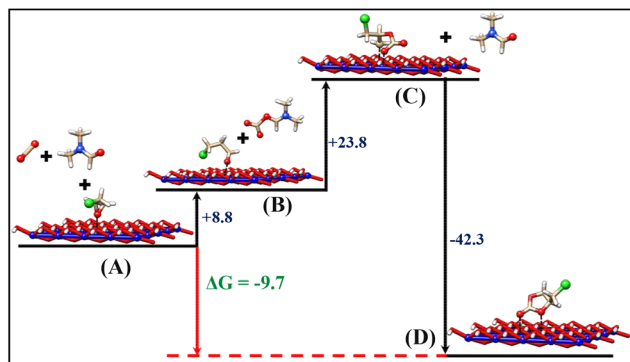


Fig. 5 Representation of the minimum geometries on the diaspore [0 4 0] surface calculated at the PBE/def2-TZVP level. The interactions between the oxygen atoms and aluminium on the sheet are indicated, along with the corresponding bond distances marked in the inset. The relative energies of the structures in the mechanism are provided along with the net free energy change for the entire reaction.

under experimental conditions. In comparison with Fig. 4, the energies shown in Fig. 5 can be analysed. Similar to the diaspore-free mechanism shown in Fig. 4, the first two steps are endergonic even in the presence of diaspore. However, there are two differences when the reaction occurs in the presence of diaspore. The extent of the rise in free energy ($32.6 \text{ kcal mol}^{-1}$) is lower compared to that in Fig. 4 ($58.9 \text{ kcal mol}^{-1}$). Furthermore, the structure C in the case of the diaspore-free mechanism is a transition state and not a stable geometry. However, in the presence of diaspore, the CO_2 is successfully transferred to the alkoxide. The final step, ring closure to form the cyclic carbonate, is associated with a negative free energy, as is the case in Fig. 4 as well. In the presence of diaspore, the net reaction has a negative total free energy ($-9.7 \text{ kcal mol}^{-1}$), indicating its spontaneity. The DMF-free mechanism is shown in ESI Fig. S27.† The free energy associated with the 3-step mechanism is $-26.6 \text{ kcal mol}^{-1}$. The negative sign indicates the spontaneity of the process even in the absence of DMF. The findings support the experimental data in which the reaction on diaspore proceeds in the absence of DMF with a yield of 58% (Table 1, entry 2). In the absence of DMF, the Al(III) ions of the diaspore activate the epoxide and the oxygen atoms of the diaspore act as the nucleophiles to open the epoxide ring.

Table 3 shows the Mulliken atomic charges on the relevant oxygen and chlorine atoms of each compound in the mecha-

nism in their unbound and bound states to the diaspore sheet. In all the structures A to D (labelled in Fig. 5), a negative charge is localised on oxygen as well as chlorine, owing to their electronegativity. The magnitude of the charge on chlorine and oxygen is not very high as these molecules are neutral species. However, evidently, the negative charges on the oxygen and chlorine atoms are reduced when these atoms bind to the aluminium in diaspore. The reduction in the negative charge confirms the charge transfer from oxygen/chlorine to the diaspore sheet. The stabilization described above is thereby attributed to the charge transfer occurring between the molecular structures and diaspore. The last row of Table 3 shows the percentage reduction in the charge before and after binding to the diaspore sheet. The oxygen atoms that are part of a ring transfer a higher percentage of charge to the diaspore as seen in structures A and D. The charge transfer is likely to ease the ring strain as electron repulsion is reduced when charge is moved away from the ring. Structure B has the advantage of the inductive effect of the alkyl chain. In structure C, the charge reduction is the least. There are two possible reasons: one of which is that oxygen is not part of a ring. The second is that the oxygen is bound to a carbon atom that is connected to two other oxygen atoms. These would compete for the electrons, thus reducing the ability of the diaspore-bound oxygen to donate electrons to aluminium. The stabilising interactions with the diaspore sheet contribute to stabilising the reaction intermediates, thereby rendering the reaction spontaneous in the presence of diaspore.

Conclusions

To summarize, this work demonstrates a simple one-pot synthesis of diaspore in aqueous medium. The as-prepared diaspore is stable in the pH range of 1 to 12 and different polar solvents such as DMSO, DCM, ethanol, and more. The results show that diaspore in the presence of a small amount of DMF is able to catalyze CO_2 fixation into multiple epoxides under atmospheric pressure with >99% selectivity. Notably, the catalyst showed excellent activity in the absence of any halide ion-containing cocatalyst. Additionally, the roles of amides such as DMF and DMAc in assisting the cycloaddition reaction have been studied. The computational results corroborate the experimental findings. The DFT calculations reveal that the overall free energy of the CO_2 insertion reaction is positive (non-spontaneous) in the absence of diaspore as there are no

Table 3 Mulliken atomic charges on the relevant oxygen atoms of each compound in the mechanism, before and after binding to the diaspore sheet. The difference in the charge before and after binding to the diaspore surface and the Al–O interaction distances are reported

Structure Atoms	Str. A	Str. B		Str. C	Str. D	
	O	O	Cl	O	O	O
Q_{O}	-0.329	-0.300	-0.203	-0.401	-0.304	-0.209
Q_{D}	-0.232	-0.219	-0.132	-0.374	-0.174	-0.090
Charge reduction	29%	27%	35%	6.7%	43%	57%

favourable interactions to stabilise the intermediates and products. However, stabilization of the structures in the diaspore sheet resulted in an overall negative (spontaneous) free energy change of the reaction. Hence, the presence of diaspore converts an otherwise non-spontaneous reaction into a spontaneous reaction owing to the interactions between the aluminium on the sheet and the substrate molecules. Overall, this study provides a feasible methodology to utilize diaspore in the presence of a small amount of DMF as a halide-free catalyst for the coupling reaction of CO₂ under mild conditions.

Author contributions

AM and VM conceptualized the idea of this work. AM and KSP carried out the synthesis and catalysis. The entire characterization was done by KSP, SG, SB and AM. The controlled experiments, substrate scope, and recyclability were analysed by AM and KSP. AR and AM performed the hot-filtration test, ICP-AES, and XPS analyses. The mechanism was proposed by VM and AC. The theoretical calculations were done by AC. The manuscript was written by AM, AC and VM. The entire work was thoroughly supervised by VM. All the authors have given approval to the final version of the manuscript.

Conflicts of interest

There are no conflicts to declare.

Acknowledgements

The authors acknowledge SERB (CRG/2022/005010-G) and IISER Kolkata for funding and instrumentation facilities, respectively. AM thanks Dr Gouri Tudu and Dr Tanmoy Biswas for their valuable suggestions. The authors also thank Shilpendu Ghosh and Souryadip Roy for helping in evaluating the pH stability. The authors thank their friends and family for their continuous support.

References

- 1 K. S. Lackner, S. Brennan, J. M. Matter, A. H. A. Park, A. Wright and B. Van Der Zwaan, The Urgency of the Development of CO₂ Capture from Ambient Air, *Proc. Natl. Acad. Sci. U. S. A.*, 2012, **109**, 13156–13162.
- 2 M. Cokoja, C. Bruckmeier, B. Rieger, W. A. Herrmann and F. E. Kühn, Transformation of Carbon Dioxide with Homogeneous Transition-Metal Catalysts: A Molecular Solution to a Global Challenge?, *Angew. Chem., Int. Ed.*, 2011, **50**, 8510–8537.
- 3 M. North, R. Pasquale and C. Young, Synthesis of Cyclic Carbonates from Epoxides and CO₂, *Green Chem.*, 2010, **12**, 1514–1539.
- 4 F. Guo and X. Zhang, Metal–Organic Frameworks for the Energy-Related Conversion of CO₂ into Cyclic Carbonates, *Dalton Trans.*, 2020, **49**, 9935–9947.
- 5 A. A. G. Shaikh and S. Sivaram, Organic Carbamates, *Chem. Rev.*, 1996, **96**, 951–976.
- 6 J. Sun, X. Yao, W. Cheng and S. Zhang, 1,3-Dimethylimidazolium-2-Carboxylate: A Zwitterionic Salt for the Efficient Synthesis of Vicinal Diols from Cyclic Carbonates, *Green Chem.*, 2014, **16**, 3297–3304.
- 7 J. Bayardon, J. Holz, B. Schäßner, V. Andrushko, S. Verevkin, A. Preetz and A. Börner, Propylene Carbonate as a Solvent for Asymmetric Hydrogenations, *Angew. Chem., Int. Ed.*, 2007, **46**, 5971–5974.
- 8 M. Peters, B. Köhler, W. Kuckshinrichs, W. Leitner, P. Markewitz and T. E. Müller, Chemical Technologies for Exploiting and Recycling Carbon Dioxide into the Value Chain, *ChemSusChem*, 2011, **4**, 1216–1240.
- 9 S. Zhang, Z. Xia, Y. Zou, F. Cao, Y. Liu, Y. Ma and Y. Qu, Interfacial Frustrated Lewis Pairs of CeO₂ Activate CO₂ for Selective Tandem Transformation of Olefins and CO₂ into Cyclic Carbonates, *J. Am. Chem. Soc.*, 2019, **141**, 11353–11357.
- 10 J. Liang, Y. B. Huang and R. Cao, Metal–Organic Frameworks and Porous Organic Polymers for Sustainable Fixation of Carbon Dioxide into Cyclic Carbonates, *Coord. Chem. Rev.*, 2019, **378**, 32–65.
- 11 C. Miceli, J. Rintjema, E. Martin, E. C. Escudero-Adán, C. Zonta, G. Licini and A. W. Kleij, Vanadium(v) Catalysts with High Activity for the Coupling of Epoxides and CO₂: Characterization of a Putative Catalytic Intermediate, *ACS Catal.*, 2017, **7**, 2367–2373.
- 12 F. Zhang, Y. Wang, X. Zhang, X. Zhang, H. Liu and B. Han, Advances in the Coupling of CO₂ and Epoxides into Cyclic Carbonates under Halogen-Free Condition, *Green Chem. Eng.*, 2020, **1**, 82–93.
- 13 F. Castro-Gómez, G. Salassa, A. W. Kleij and C. Bo, A DFT Study on the Mechanism of the Cycloaddition Reaction of CO₂ to Epoxides Catalyzed by Zn(Salphen) Complexes, *Chem. – Eur. J.*, 2013, **19**, 6289–6298.
- 14 A. Mitra, T. Biswas, S. Ghosh, G. Tudu, K. S. Paliwal, P. Ganatra and V. Mahalingam, Prudent Choice of Iron-Based Metal–Organic Networks for Solvent-Free CO₂ Fixation at Ambient Pressure, *Eur. J. Inorg. Chem.*, 2022, e202101039.
- 15 S. Das, J. Zhang, T. W. Chamberlain, G. J. Clarkson and R. I. Walton, Nonredox CO₂ Fixation in Solvent-Free Conditions Using a Lewis Acid Metal–Organic Framework Constructed from a Sustainably Sourced Ligand, *Inorg. Chem.*, 2022, **61**, 18536–18544.
- 16 G. Tudu, K. S. Paliwal, S. Ghosh, T. Biswas, H. V. S. R. M. Koppiseti, A. Mitra and V. Mahalingam, Para-Aminobenzoic Acid-Capped Hematite as an Efficient Nanocatalyst for Solvent-Free CO₂ Fixation under Atmospheric Pressure, *Dalton Trans.*, 2022, **51**, 1918–1926.
- 17 S. Subramanian, J. Park, J. Byun, Y. Jung and C. T. Yavuz, Highly Efficient Catalytic Cyclic Carbonate Formation by

- Pyridyl Salicylimines, *ACS Appl. Mater. Interfaces*, 2018, **10**, 9478–9484.
- 18 K. S. Paliwal, T. Biswas, A. Mitra, G. Tudu and V. Mahalingam, Ionic Liquid Functionalized Chitosan Catalyst with Optimized Hydrophilic/Hydrophobic Structural Balance for Efficient CO₂ Fixation, *Asian J. Org. Chem.*, 2022, **11**, e202200121.
- 19 F. Zhang, S. Bulut, X. Shen, M. Dong, Y. Wang, X. Cheng, H. Liu and B. Han, Halogen-Free Fixation of Carbon Dioxide into Cyclic Carbonates via bifunctional Organocatalysts, *Green Chem.*, 2021, **23**, 1147–1153.
- 20 R. Das and C. M. Nagaraja, Noble Metal-Free Cu(I)-Anchored NHC-Based MOF for Highly Recyclable Fixation of CO₂ under RT and Atmospheric Pressure Conditions, *Green Chem.*, 2021, **23**, 5195–5204.
- 21 N. Sharma, S. S. Dhankhar and C. M. Nagaraja, Environment-Friendly, Co-Catalyst- and Solvent-Free Fixation of CO₂ Using an Ionic Zinc(II)-Porphyrin Complex Immobilized in Porous Metal–Organic Frameworks, *Sustainable Energy Fuels*, 2019, **3**, 2977–2982.
- 22 F. Chen, N. Liu and B. Dai, Iron(II) Bis-CNN Pincer Complex-Catalyzed Cyclic Carbonate Synthesis at Room Temperature, *ACS Sustainable Chem. Eng.*, 2017, **5**, 9065–9075.
- 23 S. Chand, S. Chand, M. Mondal, S. Hota, A. Pal, R. Sahoo and M. C. Das, Three-Dimensional Co(II)-Metal–Organic Frameworks with Varying Porosities and Open Metal Sites toward Multipurpose Heterogeneous Catalysis under Mild Conditions, *Cryst. Growth Des.*, 2019, **19**, 5343–5353.
- 24 Y. Rachuri, J. F. Kurisingal, R. K. Chitumalla, S. Vuppala, Y. Gu, J. Jang, Y. Choe, E. Suresh and D. W. Park, Adenine-Based Zn(II)/Cd(II) Metal–Organic Frameworks as Efficient Heterogeneous Catalysts for Facile CO₂ Fixation into Cyclic Carbonates: A DFT-Supported Study of the Reaction Mechanism, *Inorg. Chem.*, 2019, **58**, 11389–11403.
- 25 J. Poolwong, V. Aomchad, S. Del Gobbo, A. W. Kleij and V. D'Elia, Simple Halogen-Free, Biobased Organic Salts Convert Glycidol to Glycerol Carbonate under Atmospheric CO₂ Pressure, *ChemSusChem*, 2022, **15**, e202200765.
- 26 X. Wu, C. Chen, Z. Guo, M. North and A. C. Whitwood, Metal- and Halide-Free Catalyst for the Synthesis of Cyclic Carbonates from Epoxides and Carbon Dioxide, *ACS Catal.*, 2019, **9**, 1895–1906.
- 27 J. Gao, C. Yue, H. Wang, J. Li, H. Yao, M. Y. Wang and X. Ma, CeO₂-ZrO₂ Solid Solution Catalyzed and Moderate Acidic–Basic Sites Dominated Cycloaddition of CO₂ with Epoxides: Halogen-Free Synthesis of Cyclic Carbonates, *Catalysts*, 2022, **12**, 632.
- 28 N. Bragato, A. Perosa, M. Selva and G. Fiorani, Dihydroxybenzene-Derived ILs as Halide-Free, Single-Component Organocatalysts for CO₂ Insertion Reactions, *ChemCatChem*, 2023, e202201373.
- 29 K. Liu, Z. Xu, H. Huang, Y. Zhang, Y. Liu, Z. Qiu, M. Tong, Z. Long and G. Chen, In Situ Synthesis of Pyridinium-Based Ionic Porous Organic Polymers with Hydroxide Anions and Pyridinyl Radicals for Halogen-Free Catalytic Fixation of Atmospheric CO₂, *Green Chem.*, 2022, **24**, 136–141.
- 30 A. Mitra, T. Biswas, S. Ghosh, G. Tudu, K. S. Paliwal, S. Ghosh and V. Mahalingam, Halide-Free Catalytic Carbon Dioxide Fixation of Epoxides to Cyclic Carbonates under Atmospheric Pressure, *Sustainable Energy Fuels*, 2022, **6**, 420–429.
- 31 G. P. Kharabe, N. Manna, A. Nadeema, S. K. Singh, S. Mehta, A. Nair, K. Joshi and S. Kurungot, A Pseudo-Boehmite ALOOH Supported NGr Composite-Based Air Electrode for Mechanically Rechargeable Zn-Air Battery Applications, *J. Mater. Chem. A*, 2022, **10**, 10014–10025.
- 32 B. Rezaei, Z. Hassani, M. Shahshahanipour, A. A. Ensafi and G. Mohammadnezhad, Application of Modified Mesoporous Boehmite (γ -ALOOH) with Green Synthesis Carbon Quantum Dots for a Fabrication Biosensor to Determine Trace Amounts of Doxorubicin, *Luminescence*, 2018, **33**, 1377–1386.
- 33 Z. Yang, C. Qi, X. Zheng and J. Zheng, Synthesis of Ag/ γ -ALOOH Nanocomposites and Their Application for Electrochemical Sensing, *J. Electroanal. Chem.*, 2015, **754**, 138–142.
- 34 J. Li, L. Xu, P. Sun, P. Zhai, X. Chen, H. Zhang, Z. Zhang and W. Zhu, Novel Application of Red Mud: Facile Hydrothermal-Thermal Conversion Synthesis of Hierarchical Porous ALOOH and Al₂O₃ Microspheres as Adsorbents for Dye Removal, *Chem. Eng. J.*, 2017, **321**, 622–634.
- 35 Z. Xu, J. Yu, J. Low and M. Jaroniec, Microemulsion-Assisted Synthesis of Mesoporous Aluminum Oxyhydroxide Nanoflakes for Efficient Removal of Gaseous Formaldehyde, *ACS Appl. Mater. Interfaces*, 2014, **6**, 2111–2117.
- 36 M. Barik, J. Mishra, S. Dabas, E. Chinnaraja, S. Subramanian and P. S. Subramanian, Modified Boehmite: A Choice of Catalyst for the Selective Conversion of Glycerol to Five-Membered Dioxolane, *New J. Chem.*, 2022, **46**, 695–703.
- 37 S. Liu, M. Dong, Y. Wu, S. Luan, Y. Xin, J. Du, S. Li, H. Liu and B. Han, Solid Surface Frustrated Lewis Pair Constructed on Layered ALOOH for Hydrogenation Reaction, *Nat. Commun.*, 2022, **13**, 2320.
- 38 A. Mitra, S. Ghosh, K. S. Paliwal, S. Ghosh, G. Tudu, A. Chandrasekar and V. Mahalingam, Alumina-Based Bifunctional Catalyst for Efficient CO₂ Fixation into Epoxides at Atmospheric Pressure, *Inorg. Chem.*, 2022, **61**, 16356–16369.
- 39 F. Neese, F. Wennmoths, U. Becker and C. Riplinger, The ORCA Quantum Chemistry Program Package, *J. Chem. Phys.*, 2020, **152**, 224108.
- 40 F. Neese, The ORCA Program System, *Wiley Interdiscip. Rev.: Comput. Mol. Sci.*, 2012, **2**, 73–78.
- 41 J. P. Perdew, K. Burke and M. Ernzerhof, Generalized Gradient Approximation Made Simple, *Phys. Rev. Lett.*, 1996, **77**, 3865–3868.
- 42 J. P. Perdew and Y. Wang, Accurate and Simple Analytic Representation of the Electron-Gas Correlation Energy, *Phys. Rev. B: Condens. Matter*, 1992, **45**, 13244–13249.

- 43 A. Schäfer, H. Horn and R. Ahlrichs, Fully Optimized Contracted Gaussian Basis Sets for Atoms Li to Kr, *J. Chem. Phys.*, 1998, **97**, 2571–2577.
- 44 F. Weigend and R. Ahlrichs, Balanced Basis Sets of Split Valence, Triple Zeta Valence and Quadruple Zeta Valence Quality for H to Rn: Design and Assessment of Accuracy, *Phys. Chem. Chem. Phys.*, 2005, **7**, 3297–3305.
- 45 M. Thommes, K. Kaneko, A. V. Neimark, J. P. Olivier, F. Rodriguez-Reinoso, J. Rouquerol and K. S. W. Sing, Physisorption of Gases, with Special Reference to the Evaluation of Surface Area and Pore Size Distribution (IUPAC Technical Report), *Appl. Chem.*, 2015, **87**, 1051–1069.
- 46 H. Lyu, H. Li, N. Hanikel, K. Wang and O. M. Yaghi, Covalent Organic Frameworks for Carbon Dioxide Capture from Air, *J. Am. Chem. Soc.*, 2022, **144**, 12989–12995.
- 47 S. M. Rafigh and A. Heydarinasab, Mesoporous Chitosan-SiO₂ Nanoparticles: Synthesis, Characterization, and CO₂ Adsorption Capacity, *ACS Sustainable Chem. Eng.*, 2017, **5**, 10379–10386.
- 48 A. Hakim, T. S. Marliza, N. M. Abu Tahari, R. W. N. W. Isahak, R. M. Yusop, W. M. Mohamed Hisham and A. M. Yarmo, Studies on CO₂ Adsorption and Desorption Properties from Various Types of Iron Oxides (FeO, Fe₂O₃, and Fe₃O₄), *Ind. Eng. Chem. Res.*, 2016, **55**, 7888–7897.
- 49 Z. Wang, J. Gong, J. Ma and J. Xu, In situ growth of hierarchical boehmite on 2024 aluminum alloy surface as superhydrophobic materials, *RSC Adv.*, 2014, **4**, 14708–14714.
- 50 C. Gao, X. Y. Yu, R. X. Xu, J. H. Liu and X. J. Huang, ALOOH-Reduced Graphene Oxide Nanocomposites: One-Pot Hydrothermal Synthesis and Their Enhanced Electrochemical Activity for Heavy Metal Ions, *ACS Appl. Mater. Interfaces*, 2012, **4**, 4672–4682.
- 51 S. Ghosh, R. Das, S. Kundu and M. K. Naskar, Emulsion Based Solvothermal Synthesis of CuO Grainy Rod via the Formation of Quasi-Quadrangular Prism Shaped Cu₂(OH)₃Br for Recyclable Catalyst of 4-Nitrophenol Reduction, *J. Phys. Chem. Solids*, 2020, **147**, 109551.
- 52 S. Zhang, H. Zhang, F. X. Cao, Y. Y. Ma and Y. Q. Qu, Catalytic Behavior of Graphene Oxides for Converting CO₂ into Cyclic Carbonates at One Atmospheric Pressure, *ACS Sustainable Chem. Eng.*, 2018, **6**, 4204–4211.
- 53 V. M. Lombardo, E. A. Dhulst, E. K. Leitsch, N. Wilmot, W. H. Heath, A. P. Gies, M. D. Miller, J. M. Torkelson and K. A. Scheidt, Cooperative Catalysis of Cyclic Carbonate Ring Opening: Application towards Non-Isocyanate Polyurethane Materials, *Eur. J. Org. Chem.*, 2015, 2791–2795.